Electric Field Variation in Clear and Convective Conditions at a Tropical Urban Location

Soumyajyoti Jana and Animesh Maitra

Institute of Radio Physics and Electronics, University of Calcutta, 92, A. P. C. Road, Kolkata-700009, India

mantu.abc@gmail.com, animesh.maitra@gmail.com

Corresponding Author: Animesh Maitra,
Professor, Institute of Radio Physics and Electronics
University of Calcutta,
92, Acharya Prafulla Chandra Road
Kolkata 700009, India.
Tel: +91-33-2350-9116 (Extn. 28) (Office)
Mob: +91 9433733756
Email: animesh.maitra@gmail.com
am.rpe@caluniv.ac.in

Key Points:

- Urban pollutants influence clear day atmospheric electric field at Kolkata
- PG variation increases at lower CBH and at higher LWP in the cloud
- PG variation before convective precipitation events is related with impending rain fall accumulation

This article has been accepted for publication and undergone full peer review but has not been through the copyediting, typesetting, pagination and proofreading process which may lead to differences between this version and the Version of Record. Please cite this article as doi: 10.1029/2018JD028310

Abstract

The behaviour of atmospheric electric field in terms of potential gradient (PG) has been studied during the period of 2013 and 2014 at a tropical and urban location Kolkata (22°34'N, 88°22'E), India. The clear weather PG is influenced by varying concentration of black carbon (BC) which is a major pollutant in urban atmosphere. The diurnal variation of the clear day PG follows that of the BC concentration in all the seasons. It is found that cloud base height (CBH) and liquid water path (LWP) correlate well with the PG change in convective events. It is shown that during a convective event the PG change measured over 10 min interval about 30 min before the onset of rain can approximate impending rain accumulation.

Keywords: Atmospheric electric field; black carbon; liquid water content; cloud base height; convective rain accumulation.

1 Introduction

The direct current (DC) atmospheric electric field resides between the lower ionosphere and the ground (Bennett & Harrison, 2008; Rycroft et al., 2000; Roble & Tzur, 1986; Williams, 2003; Markson, 2007). The potential difference between the lower ionosphere (~50 km during daytime) and ground drives a vertical conduction current density (1×10^{-12} Am^{-2}) to flow in all fair weather regions across the globe completing the atmospheric electrical circuit which was first proposed by Wilson (1921). Atmospheric conductivity near the earth surface arises from the ions produced by cosmic ray and terrestrial radioactivity (Bennett & Harrison, 2008; Harrison & Carslaw, 2003; Israel, 1970). The magnitude of fair-weather conduction current density is independent of height under steady-state conditions, and hence, it is varying air conductivity with height that determines the electric field vertical profile (Bennett & Harrison, 2008; Srivastava et al., 1972). By convention, the negative of the vertical component of the atmospheric electric field (E) is called potential gradient (PG),

i.e. $PG=-E$. Fair weather or cloud free conditions show positive *PG* value at ground level below 300 V/m (Bennett & Harrison, 2008; Bennett & Harrison, 2007; Dhanorkar & Kamra, 1993, 1994; Piper & Bennett, 2012). The average minimum PG value at Kolkata is ~380 V/m which vary from 350 V/m (in monsoon) to 500 V/m (in winter). The atmospheric conductivity in fair weather conditions is modulated by local atmospheric constituents like aerosols (Chalmers, 1967; Harrison & Carslaw, 2003; Piper & Bennett, 2012). This is because of the fact that the small ions become large ions after their attachments on aerosol particles which reduces their mobility (Cobb & Wells, 1970; Dhanorkar & Kamra, 1993, 1994; Harrison & Carslaw, 2003; Retalis & Retalis, 1997). The decrease in conductivity due to the reduction in ion mobility enhances the *PG* value (Cobb & Wells, 1970; Dhanorkar & Kamra, 1993, 1994; Mani & Huddar, 1972; Retalis & Retalis, 1997). Thus high pollution level (anthropogenic aerosols) increases the *PG* value at an urban location (Bennett & Harrison, 2008; Chalmers, 1967; Piper & Bennett, 2012; Sheftel et al., 1994; Silva et al., 2014).

Observations on fair weather PG over India are reported showing the effect of atmospheric pollution, smoke, and wind on the atmospheric electric field (Dhanorkar & Kamra, 1993, 1994; Guha et al., 2010; Latha, 2003; Mani & Huddar, 1972). However, the data from highly populated metropolitan cities are lacking. Also, a study of diurnal and seasonal variation of PG and BC and their interrelation is needed to have a better picture of EF variation due to different atmospheric parameters. In the present study, black carbon (BC) measurements at Kolkata ($22^{o}34'$N, $88^{o}22'$E), India, a highly polluted urban location, have been utilized to assess the impact of pollutants on atmospheric electric field. The seasonal and diurnal variation of *PG* has been investigated with respect to varying black carbon concentration which is a major pollutant aerosol at the present location. The aerosol concentration at Kolkata is considerably high showing maximum value in the winter and the minimum in the

monsoon period (Talukdar et al., 2015). Our present study intends to demonstrate the effect of pollutant particles on atmospheric electric field. This can be useful to study the pollution by monitoring atmospheric electric field.

Large variation in electric field can be observed which is associated with thick convective or shower clouds. The thunderstorms and convective events act as charge separators and modify the local atmospheric electric field near the ground (MacGorman & Rust, 1998). Charges in convective cloud are accumulated and distributed in a specific pattern (Phillips & Kintzer, 1958; Reynolds et al., 1957; Saunders, 1993; Saunders & Peck, 1998; Saunders et al., 2006). A thunderstorm has typically three charged regions, namely, upper positive, middle negative and lower small positive (Williams, 1989; MacGorman et al., 2005), forming a tripolar structure in cloud that changes the normal PG values near ground (Maitra et al., 2014).

The location of Kolkata is an urban tropical location near the land-ocean boundary. It experiences a very active monsoon and pre-monsoon period where severe convective processes are observed (Chakraborty et al., 2014, 2016; Rakshit et al., 2017). So the PG behaviour during the convective events at this location is very important. In the present study the variations of PG has been related to the cloud parameters like cloud liquid water path (LWP), cloud base height (CBH) and total rainfall amount associated with impending convective rain. Studies on electric field change on the ground in relation to convective cloud and rain are lacking in the open literature. So in the second part of the investigation, the role of convective cloud in changing the atmospheric electric field has been examined. Convective events usually occur in the afternoon period. The relationship between the cloud parameters and the electric field change near the ground has been demonstrated in the present work. This study could be useful in approximating impending rainfall amount associated with convective events by observing *PG* variation.

In this paper, Section 2 describes the data and methodology, Section 3 includes the results and Section 4 presents a discussion. The concluding remarks of the study are given in Section 5.

2 Instrumental setup, database and methodology

An electric field mill (EFM-100) operates at our site to monitor atmospheric electric field related to convective events. It uses a mechanical chopper to alternately shield and expose several sense plates to atmospheric electric field creating an AC voltage across a resistor. The magnitude of AC voltage is proportional to the amount of electric field applied to the sense plates (Bloemink, 2013; EFM-100 manual; Ferro et al., 2011). The present study utilizes the data acquired by the EFM at the rate of 2 Hz. The EFM has been mounted at the rooftop of a building and it is facing toward the roof. The rooftop values of PG are higher compared to the ground PG values. So a correction factor is calculated which is the ratio of the ground to rooftop value. The ground level data are taken by keeping EFM at the same level as the ground surface. A linear fit has been done between ground level and rooftop values of PG for clear weather conditions (MacGorman & Rust, 1998; Rakov & Uman, 2003) which yields a slope or correction factor of 0.51. The correction factor has been used to modify the rooftop EFM data for the present study.

CBH and LWP data are obtained from a microwave radiometer (RPG-HATPRO) which basically measures brightness temperature at 14 frequencies in two frequency bands, namely, 22.24-31.4 GHz (for humidity sensing) and 51.26 -58 GHz (for temperature sensing) (Rose & Czekala, 2009). Radiometer gives various products like, humidity and temperature profile, liquid water content in terms of LWP (liquid water path in g/m^2), integrated water vapor (IWV) using the brightness temperature data. RPG-HATPRO is also fitted with an IR-

Radiometer for cloud base height detection. IR radiometer can measure cloud base temperature with good accuracy (Crewell et al, 2002; Crewell & Löhnert, 2003). Now the cloud base temperature measured by IR-radiometer is combined with temperature profile measured by the microwave radiometer which provides continuous measurements with good accuracy up to 10 km. The IR-radiometer along with the microwave radiometer provides cloud base height data on a continuous basis as one of the products of the system. The radiometer can sense temperature up to 10 km with a vertical resolution of 200 m (<5000 m) and 400 m above. CBH detection accuracy is varying from 50 m (range 0-300 m) to 600m (range 5000-10000m) (Rose & Czekala, 2009; RPG-HATPRO manual).

The rain type is identified by collocated micro rain radar (MRR) which is a vertical pointing frequency modulated continuous wave (FMCW) radar at 24.1 GHz and gives drop size distributions at different heights using the Doppler spectrum of radar signal backscattered from rain drops (Peters et al., 2002). From MRR reflectivity profiles, the rain type can be classified into convective, stratiform or mixed type (Das et al., 2010; Rakshit & Maitra, 2016). The ground rain information is retrieved from an impact type disdrometer (Distromet RD-80) which senses rain drop sizes from 0.3 mm to 5.5 mm in diameter with +/-5% accuracy and 30 s temporal resolution (Disdromet, 2001).

The black carbon measurements are obtained with a 7 channel aethalometer. This instrument sucks air through a cyclone at the rate of 4 l/min which passes through a quartz filter tape. From the deposition of air particulates on the filter tape, light absorption is measured at 7 optical wavelengths (370, 470, 520, 590, 660, 880 and 950 nm) with 5 min time resolution. The 880 nm wavelength is used to measure black carbon concentration in ng/l (Talukdar et al., 2014, 2015).

The present study shows the *PG* variation during clear and convective days. The clear or fair days are identified from radiometric observation of IWV, convective available potential energy (CAPE) and MRR reflectivity profiles. In a clear day the *PG* shows only positive values indicating no overhead cloud. Also, CAPE value remains below 800 J/kg and IWV value is less than 30 mm, showing the absence of matured instability and sufficient moisture, and this can be taken as a sign of clear day (Chakraborty et al., 2016; Chakraborty & Maitra, 2016; Das & Chaudhuri, 2014; Lucas et al., 1994). We have considered 60 days of observations during the period of 2013-2014 from those clear days identified by setting above mentioned limits on CAPE, IWV and *PG*. Cloud can increase the *PG* values which can be filtered out by setting a limit on IWV and CAPE value as mentioned above (Chakraborty et al., 2016; Chakraborty & Maitra, 2016). The convective rain events are identified by the MRR reflectivity profiles showing no bright band and the rain rate exceeding 10 mm/hr.

3 Results

3.1 The diurnal variation of clear weather atmospheric electric field

The fair weather diurnal atmospheric *PG* varies according to the Carnegie curve (Aplin et al. 2008; Bauer et al. 1917; Harrison, 2013; Israel 1973a, 1973b; Mauchly 1921, 1923; Torreson et al. 1946) as shown in Figure 1a. For the present study, the PG data are averaged in each hour to show the diurnal variations in clear weather condition. Altogether 60 clear days have been considered which are distributed over the four seasons almost evenly. The diurnal data are averaged for the four seasons of 2013 and 2014 and presented with the Carnegie curve in Figure 1b. The four seasons are: i) pre-monsoon (March-May), ii) monsoon (June-September), iii) post-monsoon (October-November) and iv) winter (December-February).

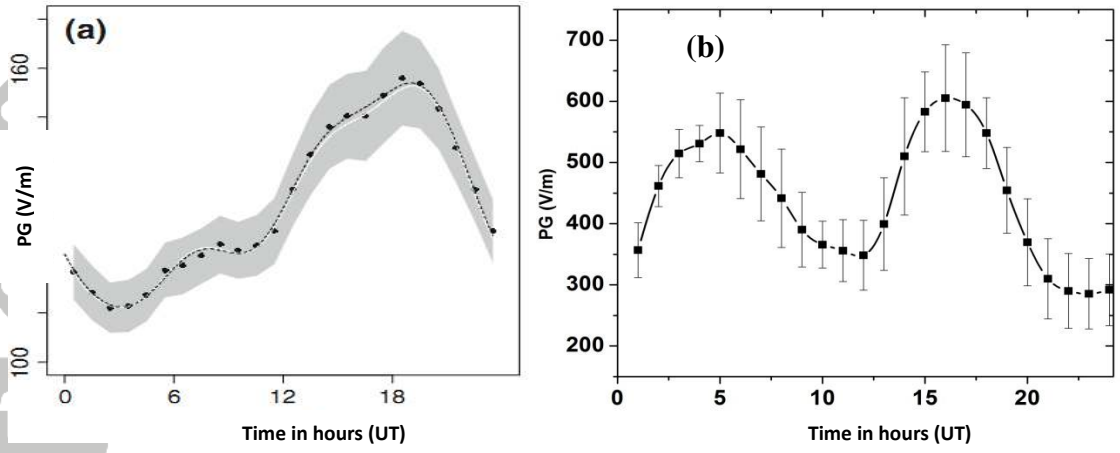

Figure 1. Comparison between (a) Carnegie curve calculated from the selected 82 undisturbed days of Cruise VII (after Harrison, 2013) and (b) PG observed at Kolkata on clear days in all seasons.

From Figure 1a it can be seen that the Carnegie curve shows only one large peak around 18 UT, whereas the diurnal variation of *PG* at the present location (Figure 1b) shows two peaks, one at 5 UT and another at 16 UT. The average *PG* values at the present location are higher than the values got from the Carnegie curve. So there is a marked difference between clear weather *PG* at present location and the *PG* observed from the Carnegie curve.

3.2 The seasonal variation of atmospheric electric field associated with black carbon

The atmospheric electric field in the fair weather condition is studied for the four seasons during the year 2013-2014 to assess the variation of *PG* with BC concentration (Figure 2). Average diurnal variation of BC concentration shows peaks in morning and evening period in all the four seasons (Figure 2a). The morning peak occurs at around 7 IST (UTC+5:30 hrs) and the evening peak at around 22 IST (Talukdar et al., 2014).

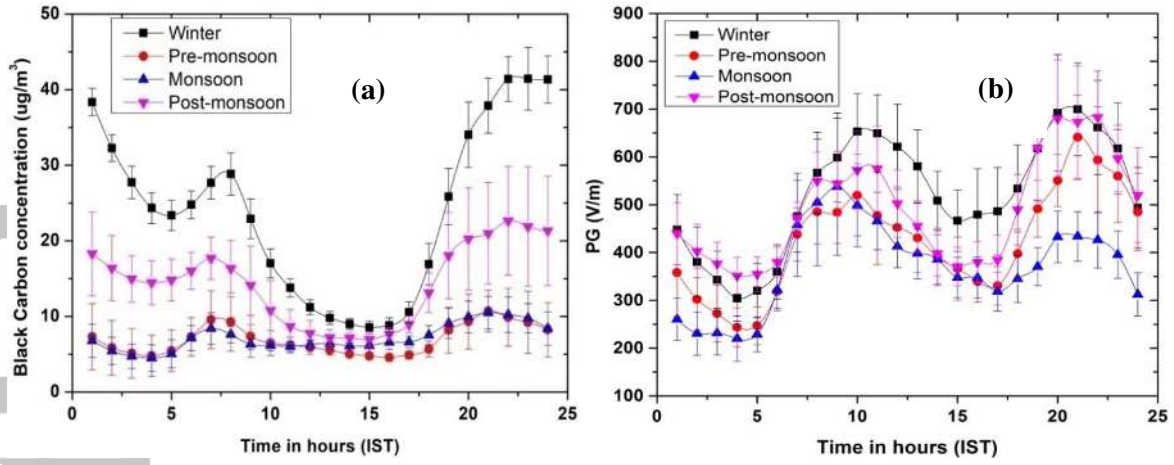

Figure 2. Seasonal variation of hourly averaged (a) BC, and (b) PG.

The seasonal variation shows maximum BC concentration during winter and minimum during monsoon and pre-monsoon period. The morning and evening peaks of BC concentration show a prominent seasonal variation as indicated in Figure 2a. It can be noted that the atmospheric electric field also shows similar diurnal pattern as the BC variation shown in Figure 2b. However, the *PG* morning peaks are delayed in respect to the BC morning peaks. Also the seasonal variation of BC values and that of the PG are generally similar (Figure 3a and b). For a comparison, the morning and evening peaks of BC and PG are plotted together in Figure 3c and d. The overall seasonal variation of the morning peaks of BC and PG show similar pattern. The standard deviation of PG value is larger in the morning than the evening in the monsoon. The evening PG values only remain in the lower segment of the morning PG values. BC peaks in morning and evening are comparable in the pre-monsoon and monsoon months. Where as evening PG in monsoon months is clearly and significantly lower than the evening PG in pre-monsoon. Moreover, the evening PG peak is higher than that morning peak in pre-monsoon months and the evening peak of PG is lower than the morning peak in the monsoon months (Figure 3c and d). Also, the evening peak values of PG are higher than the morning values of PG in winter and post-monsoon.

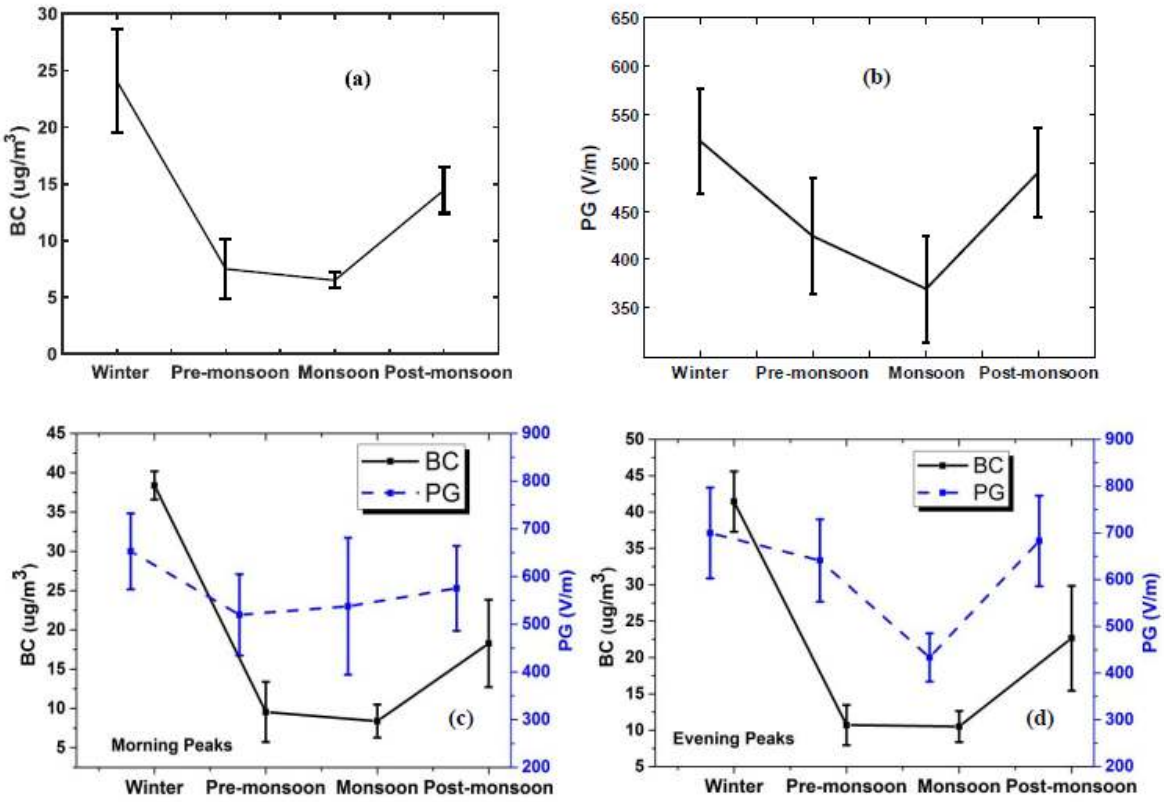

Figure 3. The average (a) BC and (b) PG values with standard deviation for all seasons and the comparison between (c) morning and (d) evening peaks of BC and PG.

The PG as well as the BC concentration is the highest (~24 µg/m^3) in dry season like winter and the lowest (~6 µg/m^3) in the wet season or monsoon due to the washout effect lingering in the clear days (Latha et al., 2005). The values of the correlation coefficient (*R*) between PG and BC, whose variations are shown in Figure 2, are obtained as: i) 0.72 for winter, ii) 0.89 for pre-monsoon, iii) 0.82 for monsoon, and iv) 0.76 for post-monsoon. The *R* values are calculated considering a time shift of 1 hour between BC and *PG* variation as we have obtained the maximum correlation for this time shift.

3.3 The variation of atmospheric electric field related to convective phenomena

Shower clouds and thunderstorms affect atmospheric PG values (MacGorman & Rust, 1998; Phillips & Kinzer, 1958; Reynolds et al., 1957; Saunders, 1993; Saunders & Peck, 1998;

Takahashi, 1978). The present study shows the influence of convective events, associated with thick convective clouds, on the PG variation in pre-monsoon and monsoon period during 2013-2014.

A typical convective event of 16 July 2013 is presented in Figure 4. The bright band signature is not observed in MRR rain rate profile, therefore, the storm is identified as a convective event, and the atmospheric electric field shows prominent variation before and during rain.

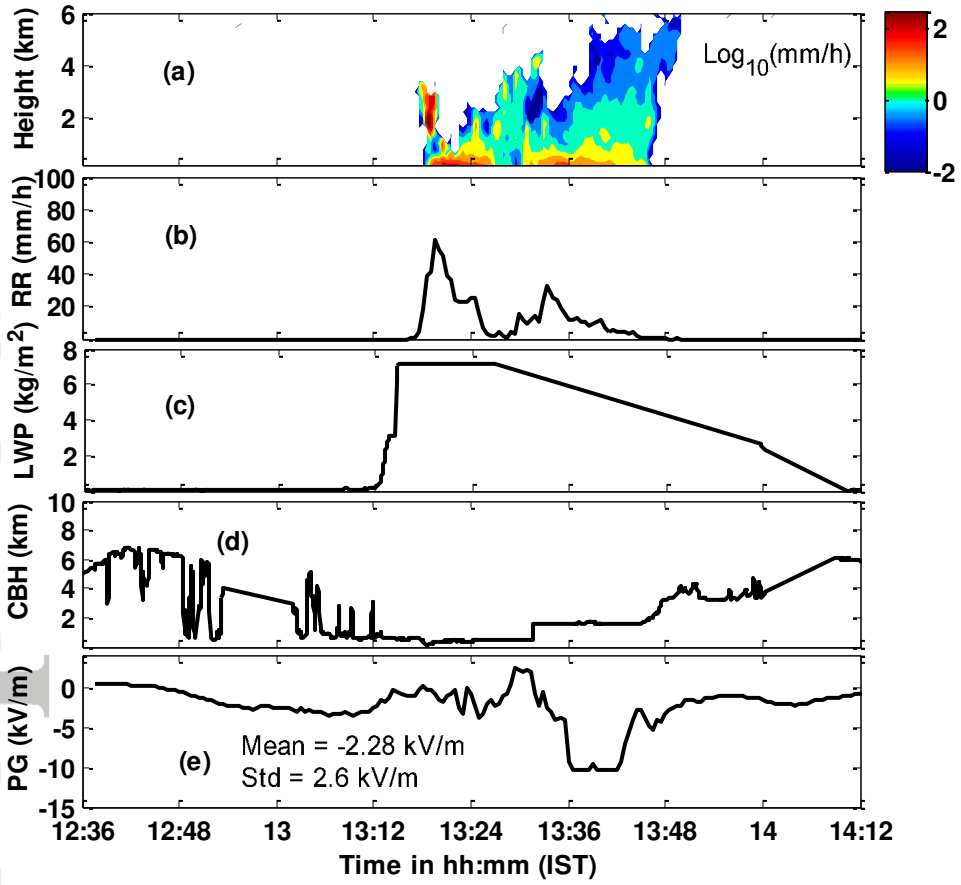

Figure 4. (a) Rain rate (RR) (mm/h) profile from MRR, (colorbar denotes the rain rate in $\log_{10}$ scale) (b) Rain rate from disdrometer, (c) LWP, (d) CBH data from radiometer, and (e) 1 min averaged electric field values during a convective event on16th July, 2013.

Figure 4a shows the rain rate profile during the event. At lower heights, rain rates are observed to be high. It may be noted that high rain attenuation prevents radar signal to reach

higher heights and get reflected. Figure 4b shows the corresponding rain rates taken from the collocated disdrometer which show a maximum rain rate of 60 mm/hr. The corresponding 1 min averaged *PG* values decrease much before the event starts which indicate presence of cloud over the EFM sensor (Figure 4e). The *PG* is averaged over every 1 min interval to remove sudden fluctuation due to lightning. After the onset of rain the *PG* shows fluctuations due to charge generation and accumulation within the cloud. Rearrangement of charges after lightning activity also creates fluctuations in the *PG* data. Rain removes charges from the cloud which also contributes to those fluctuations (Reiter, 1968). EFM shows a large negative value of PG (-10.4 kV/m) between 13:36 IST and 13:42 IST. This is the saturation value as EFM can show values up to +/- 10 kV/m. The average PG was -2.28 kV/m with a standard deviation of 2.6 kV/m. When the rain stops, the *PG* value gradually restores to normal as the cloud passes away or dissipates. The CBH shows very low values whereas LWP shows high values during the event which confirms the presence of large cloud (Figure 4c and d).

For statistical analysis the electric field data are averaged in each hour and the standard deviation is calculated to show the fluctuations during the averaging time. For the present analysis, the electric field variations during 42 days with convective events are considered. Also, convective events separated by a time gap of at least 4 hrs are considered. Usually convective rain occurs for a short duration not exceeding 1 hour (Smith et al., 2005). The present location experiences convective events in the afternoon hours. In our classification of convective days, we have taken those days where at least one convective event is present. Then the PG data are averaged in each hour and standard deviation is calculated during that hour. In this way 24 averaged PG values and corresponding standard deviations are obtained in a single convective day. Then the average and standard deviation values for 42 convective days are plotted in Figure 5c and d. A convective day may also have some periods of fair weather. The days with non-convective precipitations are not considered.

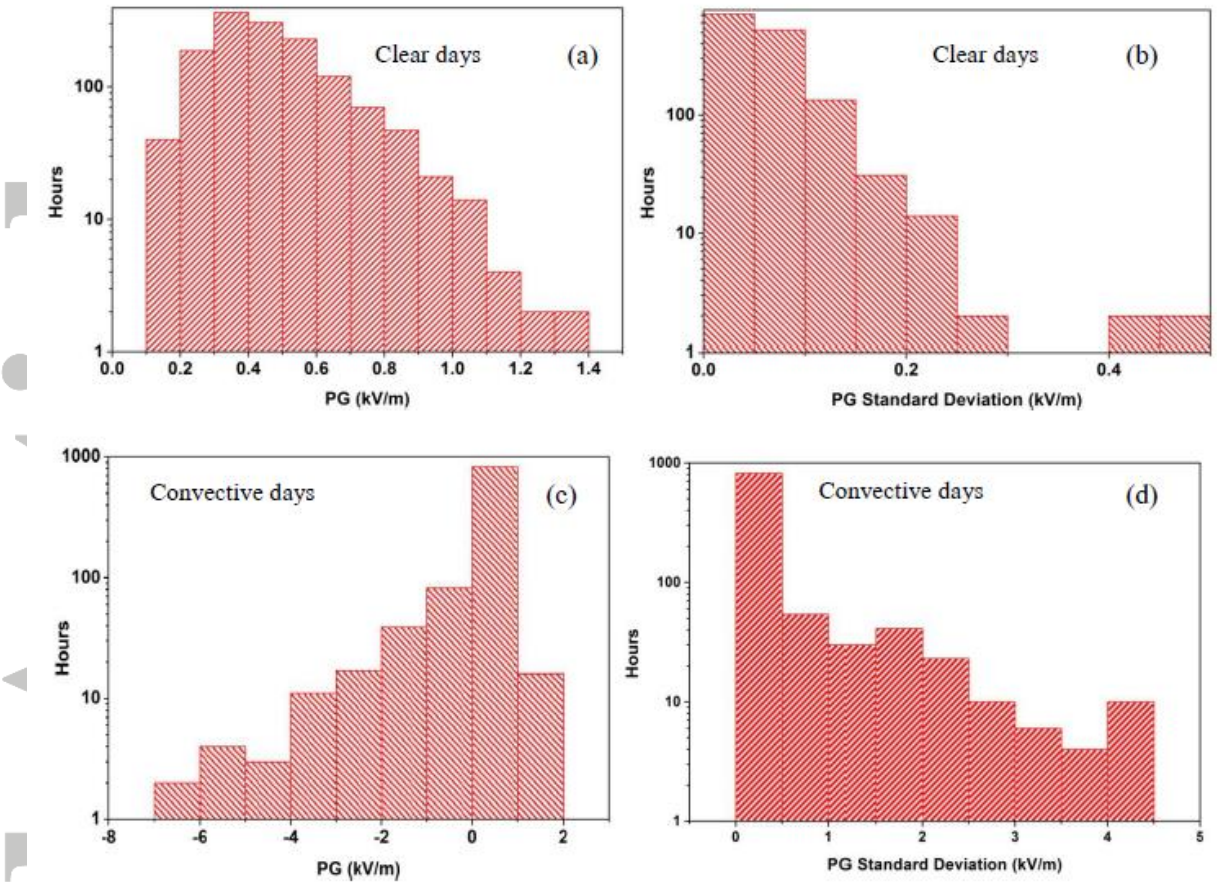

Figure 5. Hourly average of atmospheric electric field data for (a) clear days, and (c) convective days. Standard deviation about average values for (b) clear days, and (d) convective days.

In Figure 5, a comparison between the characteristics of electric field during clear days and the convective days is presented. The hourly average values of *PG* and their standard deviation (*PGSD*) are presented in Figure 5 for convective and clear days. The fluctuations created by the convective cloud are indicated by *PGSD* values which show larger values in the case of convective days. The negative *PG* values for convective days indicate the presence of clouds. On clear days the *PGSD* is small signifying the absence of cloud. Hourly averaged electric field values for clear days remain within 1.4 kV/m with a maximum standard deviation of 0.5 kV/m as shown in Figure 5a and b. With the appearance of convective cloud the electric field can take very large negative values down to -7 kV/m with standard deviation as large as 4.5 kV/m as shown in Figure 5c and d. These high negative

mean values and large standard deviations of electric field confirm large accumulation of charges in convective clouds.

Larger PGSD value classes indicate the presence of cloud and thunderstorm. As cloud is an accumulation of charges, it influences the atmospheric electric field. *PG* variation measured on the ground is influenced by the proximity of the overhead cloud, and, hence, by the value of CBH. So the hourly values of CBH and LWP from the radiometer for convective days are shown with the PGSD in Figure 6a and b.

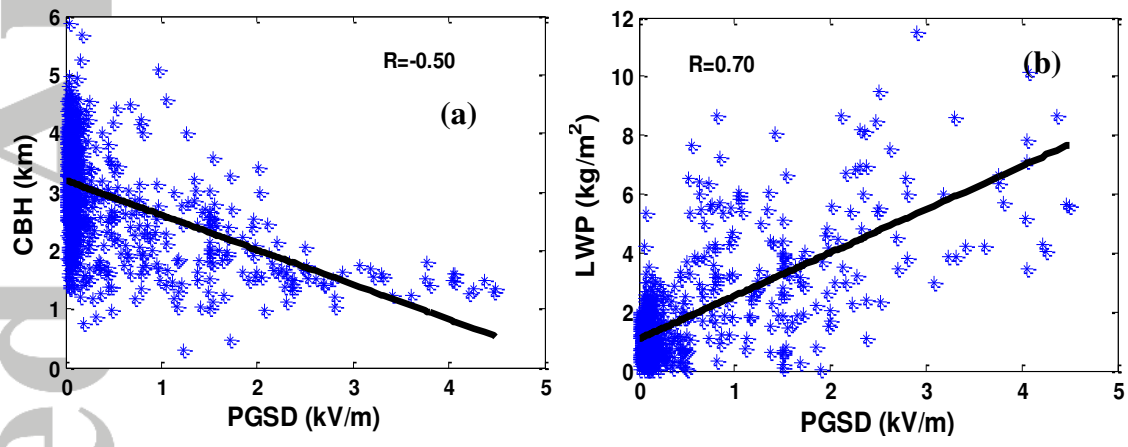

Figure 6. (a) Cloud base height, and (b) liquid water path variation with the PGSD.

Figure 6 shows that there is a negative correlation between the CBH and PGSD (R=-0.50) and a positive correlation between LWP and PGSD (R=0.70). The correlations are significant at 95% confidence level as confirmed by the t-test.

To study the behaviour of atmospheric electric field before convective events, 5 min averaged electric field is observed 3 hr prior to rain events. Figure 7 gives the average of electric field for every 5 min period prior to the 42 rain events. The start of the rain, measured by collocated disdrometer, is indicated by '0 min' on x-axis. The rapid decrease of electric field to a negative value is associated with the appearance of cloud which can be noticed 40 min prior to rain occurrence (Figure 7).

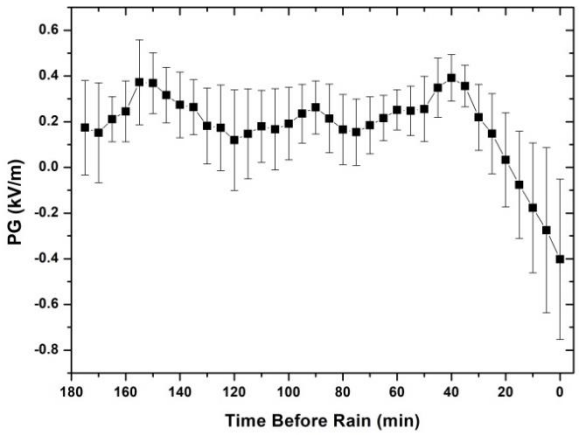

Figure 7. Average atmospheric electric field before the rain for 42 convective rain events. '0 min' indicates the start of the rain.

A definite linear relationship between liquid water content and rainfall amount exists at our location which is already reported by Chakraborty & Maitra (2012) utilizing the data from Indian Meteorological Department (IMD). As the cloud LWP has a good correlation with rain accumulation (Chakraborty & Maitra, 2012; Maitra & Chakraborty, 2018), it is expected that the change in the electric field due to cloud should also be related to the impending rain accumulation. So a relationship between the change in electric field and rainfall accumulation has been investigated. The absolute electric field change prior to rain events over an interval of 10 min (40 to 30 min before rain) has been related to the total rain accumulation within 1 hour from start of the rain for the 45 rain events. Figure 8 gives a scatter plot between electric field change 30-40 minutes before and rain accumulation. A correlation coefficient of 0.67 is obtained between the two parameters which is found to be significant at 95% confidence level by t-test.

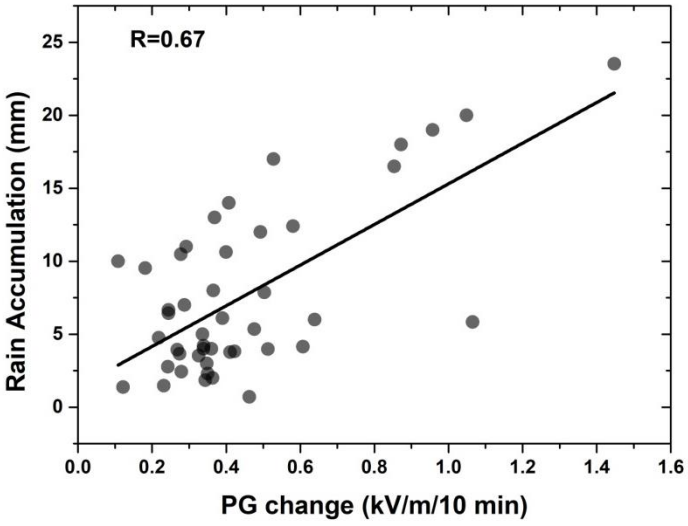

Figure 8. The scatter plot between Rain accumulations and PG changes.

4 Discussions

The present study shows the atmospheric electric field behaviour related to BC variation during fair weather and convective events. Section 3.1 shows a comparison of the yearly mean of diurnal *PG* variations (Figure 1) with the Carnegie curve for clear weather conditions. It can be seen that the Carnegie curve shows only one peak whereas the *PG* values taken at the present urban location shows two distinct peaks with higher values than that given by Carnegie curve, which is caused by the urban polluted atmosphere. Figure 2 shows the average diurnal variation of BC with standard deviation for the four seasons. There are two peaks in *PG* and BC diurnal variation which are shifted in time. The morning peaks of BC concentration shown in Figure 1 and 2 are observed due to sunrise and simultaneous increase in vehicular emissions (Stull, 1998; Talukdar et al., 2014, 2015). The inversion layer above the nocturnal boundary layer breaks with the sunrise. Pollutant particles then come down causing a short lived enhancement in BC concentration (Stull, 1988; Nair et al., 2009; Zhang et al., 2012). But since the main source of BC is vehicular emission, the morning BC peak occurs mainly because in the increase in the vehicle number which is a typical urban phenomenon. The boundary layer expansion with the increase of temperature reduces the

black carbon concentration near the surface in the noon time as shown in Figure 2a (Dumka et al., 2010; Moorthy et al., 2004; Nair et al., 2007; Talukdar et al., 2014, 2015). In the evening, BC concentration near the ground increases due to the fact that the boundary layer becomes again shallow (Kunhikrishnan et al., 1993; Raghavendra Kumar, 2011; Talukdar et al., 2014, 2015).

Pollutant particles like BC attach to the high mobility small ions and convert them to low mobility large ions (Cobb & Wells, 1970; Retalis & Retalis, 1997). The increase of large ions near the ground enhances *PG* value in the vicinity. In this way BC is responsible for the increase in the electric field. Dhanorkar and Kamra (1992) have reported on the role of small, intermediate and large ions in the variation of atmospheric conductivity in the lower atmosphere. It is reported by them that there is a delay of 1-2 hour between the morning peaks of small ions and larger ions due to time required for attachment of small ions to aerosol particles. This is the possible cause of the delay of PG peak with respect to BC peak occurring in the morning. Once the large ions disperse with the expansion of boundary layer, small ions start dominating and, thereby, reducing PG values.

Finally with boundary layer expansion, BC attached ions distributed over a large height range and PG shows low values near the ground. In the evening as boundary layer comes down along with BC particles with attached ions the *PG* increases simultaneously (Figure 2). Since ions are already attached to the BC particles, the evening peak of PG occurs quasi-simultaneously with the peak in the BC concentration without any time gap in contrast to the morning peak due to shallowness of boundary layer (Figure 2). At night time significant reduction in vehicle number and sedimentation of BC reduces BC concentration near the ground (Saha and Despiau, 2009). In this process the larger ions are reduced. On the other hand small ion concentration increases during this time by the effect of radioactive emanation

trapped under shallow boundary layer (Hoppel et al., 1986; Dhanorkar & Kamra, 1992, 1993; Kumar et al., 2016).

Regarding the seasonal variation shown in Section 3.2, the amplitudes of the morning peaks of *PG* variation appear to follow that of BC (Figure 2). There is already a general pattern of *PG* variation, shown by Carnegie curve (Harrison, 2013) showing a peak in the evening which corresponds to the second peak in the present observations. The second PG peak at the present location includes the Carnegie effect of global electric field variation which is influenced by the local BC variation pattern. This peak follows a seasonal pattern of BC at the present location as shown in Figure 3a and b. The fact that the BC concentration reduces during monsoon and pre-monsoon is also reflected in the morning peak of the *PG* variation (Figure 3c).

In general the relationship between BC concentration and PG values is based on the fact that with an increase of BC concentration the PG value increases because of the ion attachment with BC resulting in reduced conductivity. It may be noted that in the post-monsoon and winter, BC values are much higher in the evening than in the morning causing higher values of PG (Figure 3c and d). During monsoon, the standard deviation of the PG values is larger in the morning than the evening and the values measured in the evening occupy only in the lower segment of the range of values found in the morning. On the other hand, evening PG in monsoon months is lower than the evening PG in pre-monsoon, while the average BC concentration is comparable (Figure 3c and d). The correlation between PG and BC variation in different seasons (Figure 2) is about 0.7 considering one hour lag between them, the significance being already confirmed by t-test. This emphasizes the importance of *PG* measurement in monitoring the pollution level at an urban location.

Section 3.3 gives the *PG* behaviour related to convective phenomena. The convective events have a large impact on *PG* variation as the convective cloud is an accumulation of charges (Reiter, 1968). Lower CBH and higher LWP create a large PGSD value. There is a positive correlation between cloud LWP and PGSD (R=0.70) and a negative correlation between CBH and PGSD (R=-0.50). At our location convective activities are associated with high LWP, and cloud liquid water content is linearly related to rain accumulation (Chakraborty & Maitra, 2012; Maitra & Chakraborty, 2018). The statistical analysis (Figure 8) provides the evidence that the change of *PG* during 30-40 min before a convective rain event is linearly related to impending rain accumulation with root mean square error (RMSE) of 4.3 mm. This study will help in estimating the rainfall amount by monitoring of the electric field associated with convective events.

5 Conclusions

Atmospheric electric field at an urban location can be affected by pollutants under fair weather conditions and by the presence of cloud under convective weather conditions. Atmospheric electric field during clear days has a significant correlation with black carbon concentration in all the seasons. Hence, the PG value can be an indicator of the variation of the urban pollution level. Atmospheric electric field is also a good pointer of upcoming convective events. The cloud associated with a convective event has large liquid water content during pre-monsoon and monsoon months in tropical location. The cloud-induced change in atmospheric electric field is correlated to LWP and CBH. Further, a positive correlation (R=0.67) exists between atmospheric electric field change and accumulated rainfall. The change in the electric field in the timeslot 40-30 min prior to a rain event gives an estimate of impending rain accumulation.

Acknowledgements

This work is supported by the grants under the projects: (i) "Studies on aerosol environment at Kolkata located near the land-ocean boundary as a part of ARFI network under ISRO-GBP" (Grant No: SPL:GBP:ARFI:37), (ii) "UGC Basic Science Research Faculty Fellowship" (No.F.18-1/2011(BSR)), and (iii) "Space Science Promotion Scheme" (Grant No: E33013/3/2009-V). The data used in this study are available from DOI: 10.6084/m9.figshare.7461611. The Carnegie curve presented in this paper has been taken from Harrison (2013) under the Creative Commons license (http://creativecommons.org/licenses/by/4.0/). The authors are very thankful to the reviewers for their constructive comments in improving the quality of the paper.

References:

Aplin KL, Harrison, R.G., Rycroft, M.J. (2008). Investigating Earth's atmospheric electricity: a role model for planetary studies. *Space Science Revew,* 137, 11–27. doi:10.1007/s11214-008-9372-x.

Bauer, L.A., Peters, W.J., Fleming, J.A., Ault, J.P., Swann, W.F.G. (1917). Ocean magnetic observations 1905–1916 and reports on special researches, vol 3. *Researches of the Department of Terrestrial Magnetism, Carnegie Institution of Washington Publication*, 175, 378–392.

Bennett, A.J., & Harrison, R.G. (2007). Atmospheric electricity in different weather conditions. *Weather*, 62(10), 277-283.

Bennett, A.J., & Harrison, R.G. (2008). Variability in surface atmospheric electric field measurements. *Journal of Physics: Conference Series*. 142. No. 1. IOP Publishing.

Bloemink, H., (2013). Static electricity measurements for lightning warnings-an exploration. *INFRAR&D KNMI*.

Chakraborty, R., Das, S., Jana, S., & Maitra, A. (2014). Nowcasting of rain events using multi-frequency radiometric observations. *Journal of Hydrology*, 513, 467-474.

Chakraborty, R., Das, S., & Maitra, A. (2016). Prediction of convective events using multi-frequency radiometric observations at Kolkata. *Atmospheric Research,* 169, 24-31.

Chakraborty, R., Maitra, A. (2016). Retrieval of atmospheric properties with radiometric measurements using neural network. *Atmospheric Research,* 181, 124-132.

Chakraborty, S., Maitra, A. (2012). A comparative study of cloud liquid water content from radiosonde data at a tropical location. *International Journal of Geosciences*, 3(1), 44-49.

Chalmers, C. J. (1967). *Atmospheric Electricity,* pp. 168–169, 188, Pergamon Press, London.

Cobb, W. E., & Wells, H. J. (1970). The electrical conductivity of oceanic air and its correlation to global atmospheric pollution. *Journal of the Atmospheric Sciences*, 27(5), 814-819.

Crewell, S., Drusch, M., Van Meijgaard, E., & Van Lammeren, A. C. A. P. (2002). Cloud observations and modeling within the European BALTEX cloud liquid water network. *Boreal environment research*, *7*(3), 235-246.

Crewell, S., & Löhnert, U. (2003). Accuracy of cloud liquid water path from ground-based microwave radiometry 2. Sensor accuracy and synergy. *Radio Science*, *38*(3), 7-1.

Das, D., & Chaudhuri, S. (2014). Remote sensing and ground-based observations for nowcasting the category of thunderstorms based on peak wind speed over an urban station of India. *Natural hazards*, 74(3), 1743-1757.

Das, S., Shukla, A. K., & Maitra, A. (2010). Investigation of vertical profile of rain microstructure at Ahmedabad in Indian tropical region. *Advances in Space Research,* 45(10), 1235-1243.

Dhanorkar, S., & Kamra, A. K. (1992). Relation between electrical conductivity and small ions in the presence of intermediate and large ions in the lower atmosphere. *Journal of Geophysical Research: Atmospheres*, 97(D18), 20345-20360.

Dhanorkar, S. & Kamra, A. K. (1993) Diurnal and seasonal variations of the small-, intermediate-, and large-ion concentrations and their contributions to polar conductivity, *Journal of Geophysical Research: Atmospheres*, 98(D8), 14895–14908.

Dhanorkar, S. & Kamra, A. K. (1994). Diurnal variation of ionization rate close to ground. *Journal of Geophysical Research: Atmospheres*, 99(D9), 18523–18526, 1994.

Dumka, U.C., & Moorthy, K. K. (2010). Characteristics of aerosol black carbon mass concentration over a high altitude location in the Central Himalayas from multi-year measurements. *Atmospheric Research,* 96, 510–521.

Distromet, L. T. D., (2001). Disdrometer RD-80: Instruction Manual. Distromet LTD, Basel, Switzerland.

EFM-100 Atmospheric Electric Field Monitor, Installation/Operators Guide. (http://www.boltek.com/EFM-100_Manual_03102015.pdf)

Ferro, M., Yamasaki, J., Pimentel, D. R. M., Naccarato, K. P., & Saba, M. M. (2011). Lightning risk warnings based on atmospheric electric field measurements in Brazil. *Journal of Aerospace Technology and Management*, 3(3), 301-310.

Guha, A., De, B. K., Gurubaran, S., De, S. S., & Jeeva, K. (2010). First results of fair-weather atmospheric electricity measurements in Northeast India. *Journal of earth system science*, 119(2), 221-228.

Harrison, R. G. (2013). The Carnegie curve. *Surveys in Geophysics*, 34(2), 209-232.

Harrison, R. G., & Carslaw, K. S. (2003). Ion- aerosol- cloud processes in the lower atmosphere. *Reviews of Geophysics*, 41(3).

Hoppel, W. A., Anderson, R. V., & Willett, J. C. (1986). Atmospheric electricity in the planetary boundary layer. *The Earth's Electrical Environment*, Washington, DC, USA: National Academy Press, 149-165.

Israel, H. (1970). *Atmospheric Electricity. Vol. L Fundamentals, conductivity, ions,* Israel Program for Scientific Translations Jerusalem, 106-110.

Israel, H. (1973a). Atmospheric Electricity, vol. I, Fundamentals, Conductivity, Ions, Published for the National Science Foundation by the Israel Program for Scientific Translations, ISBN 0 7065 1129 8.

Israel, H. (1973b). Atmospheric Electricity, vol. II Fields, Charges and Currents, Published for the National Science Foundation by the Israel Program for Scientific Translations, ISBN 0 7065 1129 8.

Kumar, K. C., Prasad, T. R., Ratnam, M. V., & Nagaraja, K. (2016). Activity of radon (222Rn) in the lower atmospheric surface layer of a typical rural site in south India. *Journal of Earth System Science*, *125*(7), 1391-1397.

Kunhikrishnan, P.K., Gupta, K.S., Ramachandran, R., Prakash, J.W., & Nair, K.N. (1993). Study on thermal internal boundary layer structure over Thumba, India. *Annales geophysicae,* 11 (1), 52–60.

Latha, R. (2003). Diurnal variation of surface electric field at a tropical station in different seasons: a study of plausible influences. *Earth, planets and space*, *55*(11), 677-685.

Latha, K. M., Badarinath, K. V. S., & Reddy, P. M. (2005). Scavenging efficiency of rainfall on black carbon aerosols over an urban environment. *Atmospheric Science Letters,* 6(3), 148-151.

Lucas, C., Zipser, E. J., & LeMone, M. A. (1994). Convective available potential energy in the environment of oceanic and continental clouds; correction and comments. *Journal of the Atmospheric Sciences*, 51(24), 3829-3830.

MacGorman, D. R., Rust, W. D., Krehbiel, P., Rison, W., Bruning, E., & Wiens, K. (2005). The electrical structure of two supercell storms during STEPS. *Monthly weather review,* 133(9), 2583-2607.

MacGorman, D. R., & Rust, W. D. (1998). *The electrical nature of storms*. Oxford University Press on Demand.

Maitra, A., & Chakraborty, R. (2018). Prediction of Rain Occurrence and Accumulation Using Multifrequency Radiometric Observations. *IEEE Transactions on Geoscience and Remote Sensing*. 56, 2789-2797.

Maitra, A., Jana, S., Chakraborty, R., & Majumder, S. (2014). *Multi-technique observations of onvective rain events at a tropical location*. In General Assembly and Scientific Symposium (URSI GASS), 2014 XXXIth URSI, 1-4, IEEE.

Mani, A., & Huddar, B. B. (1972). Studies of surface aerosols and their effects on atmospheric electric parameters. *Pure and Applied Geophysics,* 100, 154–156.

Markson, R. (2007). The global circuit intensity: its measurement and variation over the last 50 years. *Bulletin American Meteorological Society*. doi:10.1175/BAMS-88-2- 223, 223-241.

Mauchly, S.J. (1921). Note on the diurnal variation of the atmospheric electric potential gradient. *Physical Reveiw*, 18, 161–162.

Mauchly, S.J. (1923). On the diurnal variation of the potential gradient of atmospheric electricity. *Terr Magn*, 28, 61–81.

Moorthy, K. K., Babu, S. S., Sunilkumar, S. V., Gupta, P. K., & Gera, B. S. (2004). Altitude profiles of aerosol BC, derived from aircraft measurements over an inland urban location in India. *Geophysical Research Letter*, 31 (L22103). http://dx.doi.org/10.1029/2004GL021336.

Nair, P. R., George, K. S., Parameswaran, K., Aloysius, M., Alappattu, D. P., Mohan, M., & Kunhikrishnan, P. K. (2009). Short-term changes in the aerosol characteristics at Kharagpur (22° 19′ N, 87° 19′ E) during winter. *Journal of Atmospheric and Solar-Terrestrial Physics*, 71(17-18), 1771-1783.

Nair, V.S., Moorthy, K.K., Alappattu, D.P., Kunhikrishnan, P.K., George, S., Nair, P.R., Babu, S.S., Abish, B., Satheesh, S.K., Tripathi, S.N. & Niranjan, K. (2007). Wintertime aerosol characteristics over the Indo- Gangetic Plain (IGP): Impacts of local boundary layer processes and long- range transport. *Journal of Geophysical Research: Atmospheres*, 112(D13). http://dx.doi.org/10.1029/2006JD008099.

Peters, G., Fischer, B., & Andersson, T. (2002). Rain observations with a vertically looking Micro Rain Radar (MRR). *Boreal Environment Research, 7*(4), 353-362.

Phillips, B. B., & Kinzer, G. D. (1958). Measurements of the size and electrification of droplets in cumuliform clouds. *Journal of Meteorology,* 15.4, 369-374.

Piper, I. M., & Bennett. A. J. (2012). Observations of the atmospheric electric field during two case studies of boundary layer processes. *Environmental Research Letters*, 7.1: 014017.

Raghavendra Kumar, K. (2011). Characterization of aerosol black carbon over a tropical semi-arid region of Anantapur, India. *Atmospheric Research,* 100, 12–27.

Roble, R.G., & Tzur, I. (1986). *The global atmospheric–electrical circuit. The Earth's Electrical Environment*. National Academy Press.

Rakshit, G., & Maitra, A. (2016). Simultaneous Radar Observations of Vertical Profile of Rain Features from Space and Ground at Ku and Ka Bands at a Tropical Location. *MAPAN*. 31.4, 291-297.

Rakshit, G., Adhikari, A., & Maitra, A. (2017). Modelling of Rain Decay Parameter for Attenuation Estimation at a Tropical Location. *Advances in Space Research,* 59.12, 2901-2908.

Rakov, V. A., Uman, M. A. (2003). *Lightning Physics and Effects.* Cambridge University Press.

Reynolds, S. E., Brook, M., & Gourley, M. F. (1957). Thunderstorm charge separation. *Journal of Meteorology,* 14.5, 426-436.

Reiter, R. (1968). Results of investigation on precipitation and cloud electricity based on 15 years of observation. *Archiv für Meteorologie, Geophysik und Bioklimatologie, Serie A*, 17(1), 17-29.

Retalis, D., & Retalis, A. (1997). The atmospheric electric field in Athens-Greece. *Meteorology and Atmospheric Physics,* 63(3), 235-241.

Rose, Th, & Czekala, H. (2009). *RPG-HATPRO Radiometer Operating Manual*. Radiometer Physics GmbH.

Rycroft, M. J., Israelsson, S., & Price, C. (2000). The global atmospheric electric circuit, solar activity and climate change. *Journal of Atmospheric and Solar-Terrestrial Physics,* 62(17), 1563-1576.

Saha, A., & Despiau, S. (2009). Seasonal and diurnal variations of black carbon aerosols over a Mediterranean coastal zone. *Atmospheric Research*, *92*(1), 27-41.

Saunders, C. P. R. (1993). A review of thunderstorm electrification processes. *Journal of Applied Meteorology,* 32.4, 642-655.

Saunders, C. P. R., & Peck, S. L. (1998). Laboratory studies of the influence of the rime accretion rate on charge transfer during crystal/graupel collisions. *Journal of Geophysical Research: Atmospheres,* 103(D12), 13949-13956.

Saunders, C. P. R., Bax-Norman, H., Emersic, C., Avila, E. E., & Castellano. N. E. (2006). Laboratory studies of the effect of cloud conditions on graupel/crystal charge transfer in thunderstorm electrification. *Quarterly Journal of the Royal Meteorological Society,* 132, 621, 2653-2674

Sheftel, V. M., Chernyshev, A. K., & Chernysheva, S. P. (1994). Air conductivity and atmospheric electric field as an indicator of anthropogenic atmospheric pollution. *Journal of Geophysical Research: Atmospheres,* 99(D5), 10793-10795.

Silva, H. G., Conceição, R., Melgão, M., Nicoll, K., Mendes, P. B., Tlemçani, M., Heitor Reis, A., & Harrison, R. G. (2014). Atmospheric electric field measurements in urban environment and the pollutant aerosol weekly dependence. *Environmental Research Letters*, 9(11), 114025.

Smith, J. A., Miller, A. J., Baeck, M. L., Nelson, P. A., Fisher, G. T., & Meierdiercks, K. L. (2005). Extraordinary flood response of a small urban watershed to short-duration convective rainfall. *Journal of Hydrometeorology*, 6(5), 599-617.

Srivastava, G. P., Huddar, B. B., & Mani, A. (1972). Electrical conductivity and potential gradient measurements in the free atmosphere over India. *Pure and Applied Geophysics*, 100(1), 81-93.

Stull, R. B. (1998). *An introduction to boundary layer meteorology*. Kluwer Academic Publishers, Dordrecht.

Takahashi, T. (1978). Riming electrification as a charge generation mechanism in thunderstorms. *Journal of the Atmospheric Sciences,* 35(8), 1536-1548.

Talukdar, S., Jana, S., & Maitra, A. (2014). Variation of black carbon concentration associated with rain events at a tropical urban location. *Current Science,* 106, 1.

Talukdar, S., Jana, S., Maitra, A., & Gogoi, Mukunda M. (2015). Characteristics of black carbon concentration at a metropolitan city located near land–ocean boundary in Eastern India. *Atmospheric Research,* 153, 526-534.

Torreson, O.W., Parkinson, W.C., Gish, O.H., Wait, G.R. (1946). Ocean atmospheric-electric results (Scientific Results of Cruise VII of the Carnegie during 1928–1929 under command of Captain J. P. Ault, vol 3). *Researches of the Department of Terrestrial Magnetism. Carnegie Institution of Washington Publication*, vol. 568.

Williams, E. R. (1989). The tripole structure of thunderstorms. *Journal of Geophysical Research: Atmosphere,* 94(D11), 13151-13167.

Williams, E.R. (2003). The global electrical circuit. In: Holton, J.R., Pyle, J., Curry, J.A. (Eds.), Encyclopedia of Atmospheric Sciences, vol. 2. Elsevier, 724–732.

Wilson, C. T. R. (1906). On the Measurement of the Earth-Air Current and on the Origin of Atmospheric Electricity. Cambridge Proc. Phil. Soc. 13(6), 363-382.

Wilson, C. T. R. (1921). Investigations on lightning discharges and on the electric field of thunderstorms. *Philosophical Transactions of the Royal Society of London. Series A, Containing Papers of a Mathematical or Physical Character,* 221, 73-115.

Zhang, X., Huang, Y., & Rao, R. (2012). Aerosol characteristics including fumigation effect under weak precipitation over the southeastern coast of China. *Journal of Atmospheric and Solar-Terrestrial Physics*, 84, 25-36.